



Efficient and ultraviolet durable inverted polymer solar cells using thermal stable GZO-AgTi-GZO multilayers as a transparent electrode

Xuanhuai Lin ^a, Hui Luo ^a, Xiangkun Jia ^a, Jinfeng Wang ^a, Jianping Zhou ^b, Ziyao Jiang ^a, Likun Pan ^a, Sumei Huang ^a, Xiaohong Chen ^{a,*}

^a Engineering Research Center for Nanophotonics and Advanced Instrument, Ministry of Education, and School of Physics and Materials Science, East China Normal University, Shanghai 200062, China

^b School of Automation Engineering, Shanghai University of Electric Power, Shanghai 200092, China



ARTICLE INFO

Article history:

Received 27 August 2016
Received in revised form
18 September 2016
Accepted 6 October 2016

Keywords:

Polymer solar cells
Thermal stability
UV durability
Ag
Transparent conducting films

ABSTRACT

The optical and electrical properties of GZO/AgTi/AZO (GATG) multilayer transparent conducting films fabricated by magnetron sputtering method were investigated. The sheet resistance and maximum optical transmittance of GATG films are 5 Ω/sq and 86%, respectively. The sheet resistance of GATG still retains stable under annealing at 400 °C, which shows better thermal stability compared to GZO/Ag/AZO (GAG) film. The enhanced thermal stability of GATG is attributed to the formation of TiO_x in Ti doped Ag nanostructure film, which can inhibit Ag atom diffusion and aggregation. PTB7-TH:PC₇₁BM based inverted polymer solar cells (PSCs) with GATG electrode gave PCE of 9.20%, which is comparable to PCE (9.23%) of the control PSCs with ITO electrode. The PCE of PSCs with GATG and ITO electrodes respectively remain 59% and 23% of the original PCE values after UV exposure for 20 min with relativize humidity of 68% in air, indicating that PSCs with GATG show better UV durability. Our results suggest that GATG as an alternative to ITO electrode can obtain efficient inverted PSCs and have stronger anti-UV ability due to its low UV transparency.

© 2016 Elsevier B.V. All rights reserved.

1. Introduction

Recently, significant progresses in polymer organic solar cells (PSCs) have been made obtaining solution-processed single junction PSCs with power conversion efficiency (PCE) over 9% [1]. The comprehensive performance of polymer solar cells including PCE, stability and cost still need be further improved to meet the commercial application. The wide use of indium-tin-oxide (ITO) transparent electrode in optoelectronic devices is gradually pushing up the cost of ITO electrode because indium is not abundant on Earth. Therefore, developing the efficient and inexpensive transparent electrode substituting ITO electrode in PSCs helps to maintain the potential low cost advantage of PSCs. A variety of ITO replacements have been investigated, including poly(3,4-ethylenedioxylenethiophene):poly(styrenesulphonic acid) (PEDOT:PSS), graphene, metal grid lines, impurity doped-ZnO and metal based sandwiched structure transparent conducting films [2–5]. Among them, ZnO has obtained significant attention due to

its advantages of abundance in nature and nontoxicity. The low resistance and high transparent films based on impurity doped-ZnO can be obtained and are considered a possible alternative to ITO electrode [6–8]. PSCs based on AZO (Al doped ZnO) electrode compared to ITO electrode can significantly enhance the ultraviolet (UV) durability because of UV filtering role of AZO electrode [9]. Metal based sandwiched structure transparent conducting film, metal oxide/metal/metal oxide (OMO) [10,11], are also considered a possible alternative to ITO because of its superior properties of the low sheet resistance and high optical transmittance. The ~100 nm total thickness of AZO/Ag/AZO can easily reach ~5 Ω/sq sheet resistance with the maximum optical transmittance of more than 85% [12]. The AZO film usually need be deposited ~1 μm thickness to obtain ~10 Ω/sq sheet resistance and is difficult to further decrease sheet resistance for retaining high optical transmittance [13]. Therefore, the typical structure transparent electrodes such as AZO/Ag/AZO compared to AZO electrode are more easily obtained the lower sheet resistance (~5 Ω/sq) while still keeping high optical transmittance.

The electrical and optical properties of metal based sandwiched structure transparent conducting films have been wildly investigated, where the typical sandwiched metals are, for examples Cu

* Corresponding author.

E-mail address: xhchen@phy.ecnu.edu.cn (X. Chen).

[14], Ag, Au [15], Ni [16], and Mo [17]. However, the noble metals Ag and Au compared to the cheap metals show more superior comprehensive properties, such as lower resistance, stability and optical transmittance. Au metal has marvelous electrical and optical properties, but its expensive cost would limit the massive application. Ag metal has superior conducting and optical properties and shows the reasonable cost, which is a right sandwiched metal in OMO films [18]. The Ag based multilayer transparent conducting films such as zinc tin oxide (ZTO)/Ag/ZTO (ZAZ) and AZO/Ag/AZO, fabricated with magnetron sputtering deposition can obtain sheet resistance of $\sim 5 \Omega/\text{sq}$ and average transmittance over 80% in the visible light range, which is almost comparable to that of ITO films with the $\sim 5 \Omega/\text{sq}$ sheet resistance [19].

The Ag based multilayer transparent conducting electrodes as an alternative to ITO electrode have been applied to solar cells [20,21]. Semitransparent inverted polymer solar cells (PSCs) was developed by thermally evaporated $\text{MoO}_3/\text{Ag}/\text{MoO}_3$ as transparent anode [22]. PSCs with Ag based multilayer electrodes, such as (Ga doped ZnO) GZO/Ag/GZO, AZO/Ag/AZO, fabricated with magnetron sputtering deposition, have almost obtained the comparable power conversion efficiency (PCE) of PSCs with ITO electrode. Furthermore, PSCs with Ag based multilayer electrode have superior resistance bending compared to PSCs with ITO and AZO electrodes due to the excellent ductility of Ag film [23]. However, the stability of Ag based multilayer transparent conducting films still need be further improved during annealing and aging to meet the industrial application. The sandwiched Ag film is unstable because Ag atoms can gradually be aggregated and/or diffused into the adjoining layers during annealing and aging, which would deteriorate the optical and electrical properties of OMO electrodes [24,25]. To inhibit Ag atoms aggregation and diffusion, we previously developed five-layer structure AZO/Al/Ag/Al/AZO multilayer electrode [12]. The thermal stability of Ag based multilayer transparent conducting film was greatly improved because the inserted Al thin film inhibits Ag atoms diffusion and aggregation. Furthermore, the PCE of PSCs with five-layer structure Ag based electrode is comparable to that of the control PSCs with ITO electrode. However, the five-layer structure electrode increases the procedure complexity and the fabrication cost. In this paper, we further develop Ti doped Ag alloy instead of pure Ag fabricating GZO/AgTi/GZO (GATG) film, which can efficiently simplify the fabricated procedure and improve its thermal stability. The PCE values of PSCs with GATG transparent electrode is comparable to that of PSCs with ITO. Furthermore, the UV durability of PSCs based on GATG electrode is significantly enhanced compared to the control PSCs with ITO electrode.

2. Experimental section

Glass substrates ($2.5 \times 2.5 \text{ cm}^2$) were cleaned with deionized water, acetone, methanol and isopropanol for 20 min per cleaning agent in an ultrasonic bath, blown with N_2 stream and dried at 140°C for 30 min in the oven, finally underwent ultraviolet-ozone treatment for 20 min. GZO, AgTi and GZO layers were consecutively deposited onto glass substrates by a DC magnetron sputtering system. The purities of GZO and Ag targets are both 99.9%. GZO corresponds to a ZnO target doped with 3.0 wt% Ga_2O_3 . A few Ti pieces or wires were attached on the Ag target to fabricate Ti doped Ag film. The atom percentage of Ti in AgTi film is about 0.5 at% [26]. The sputtering Ar flow rate and gas pressure were respectively 15 sccm and 0.3 Pa with the base pressure of $3 \times 10^{-3} \text{ Pa}$.

PSCs, with structures of ITO or GATG/ZnO/PTB7-Th:PC₇₁BM/ MoO_3/Ag , were fabricated. The cleaned ITO/glass and GATG/glass substrates were treated with ultraviolet ozone for 15 min, followed by spin coating ZnO electron transport layer and then annealing at

150°C for 30 min in air. The sol-gel ZnO nanoparticles were synthesized following the procedures described in previous publications [27,28]. In a typical synthesis, a stoichiometric amount of tetramethylammonium hydroxide dissolved in ethanol (0.5 M) was dropped wisely into 0.1 M zinc acetate dihydrate dissolved in dimethyl sulfoxide (DMSO), followed by stirring for 1 h at room temperature. After being washed with hexane and ethanol (2:1) mixing solvents, ZnO nanoparticles were dispersed in ethanol. Then sol-gel ZnO solutions were spin coated at 4000 rpm for 50 s onto ITO or GATG films to form 20 nm films, followed by annealing at 150°C for 30 min in air. PTB7-Th (99%) was purchased from 1-Material INC. and PC₇₁BM (99.5%) was purchased from Solenne BV. An 80 nm thick active layer was spin coated on the ZnO surface using a blended solution containing PTB7-Th:PC₇₁BM (7 mg/mL:10.5 mg/mL) dissolved in chlorobenzene/1,8-diiodooctane (97:3, v/v) at 1000 rpm for 15 s in argon-filled glovebox. A 7 nm thick MoO_3 interlayer and a 100 nm thick Ag were successively thermally evaporated onto the PTB7-Th:PC₇₁BM photoactive layer with a base pressure of $3 \times 10^{-4} \text{ Pa}$. The J-V characteristics of PSCs were measured by a Keithley 2440 Sourcemeter together with a Newport solar simulator with an AM1.5G illumination of 100 mW/cm² calibrated with a standard silicon reference cell. The incident photon to current conversion efficiency (IPCE) of PSCs was measured over the wavelength range from 300 nm to 800 nm using a Newport Optical Power Meter 2936-R. Sheet resistance measurements were performed using the four-point probe technique. The optical transmittance and absorption spectra were measured using a UV–Vis–NIR spectrometer (UV3900, Unicam). The surface morphologies of samples were investigated by field-emission scanning electron microscopy (FESEM, Hitachi S-4800).

3. Results and discussion

The optical transmittance of GAG and GATG is not only related to the thickness of bottom and top GZO layer [29], but also dependent on the thickness of the Ag layers due to the surface plasmon resonance effect of Ag film [2,23]. Fig. 1a the optical transmittance spectra of GATG and GAG transparent conducting films. The optical transmittance and shapes of GATG films was varied with the thickness of Ti doped Ag film. The maximum optical transmittance of GATG film can reach 86% with 10 nm Ti doped Ag film, and corresponds to the sheet resistance of about $5 \Omega/\text{sq}$. The average sheet resistance of GATG films was decreased from $16 \Omega/\text{sq}$ to $3 \Omega/\text{sq}$ with increasing Ag thickness from 8 to 16 nm, as shown in Fig. 1b, indicating that the sheet resistance of GATG films is primarily determined by the Ti doped Ag film [30]. This is because the electrical resistivity of Ag film is far lower than of metal oxides [23,31]. The low transmittance at the Ag thickness of 8 nm is attributed to the impacting surface morphology of Ag islands which increases the absorption of incident light and makes the contribution to decrease the transmittance [2,32], while low transmittance at the Ag thickness of 16 nm is blamed for reducing interface effects between Ag layer and top/bottom thin films [31]. The optimized GZO(40 nm)/AgTi(10 nm)/GZO(40 nm) and GZO(40 nm)/Ag(12 nm)/GZO(40 nm) films obtain the sheet resistance of $\sim 5 \Omega/\text{sq}$, and optical transmittance of 86% and 82%, respectively.

Fig. 2 (a) and (b) show the optical transmittance spectra of GAG and GATG films with difference annealing temperature. The optical transmittance spectra of GATG films still retain stable under annealing respectively at 430°C and 450°C for 30 min. However, the optical transmittance of GAG film were significantly reduced in the wavelength range from 500 nm to 800 nm, indicating the morphologies of inserted Ag nanostructure film have been varied under annealing at 450°C for 30 min, which would affect the

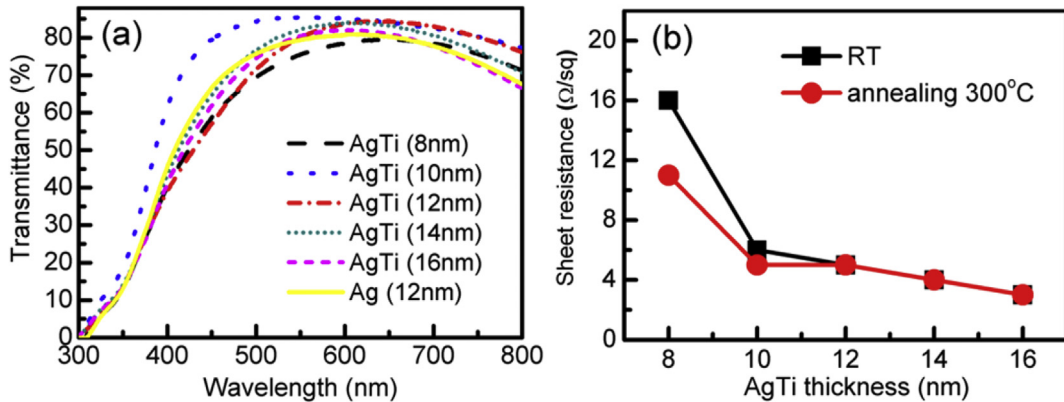


Fig. 1. (a) Transmittance spectra of transparent conducting films with the structure: GZO(40 nm)/AgTi(Xnm)/GZO(40 nm) and GZO(40 nm)/Ag(12 nm)/GZO(40 nm). (b) Sheet resistance of GZO(40 nm)/AgTi(Xnm)/GZO(40 nm) with different nominal thickness of AgTi films. Annealing condition is 300 °C for 30 min in air.

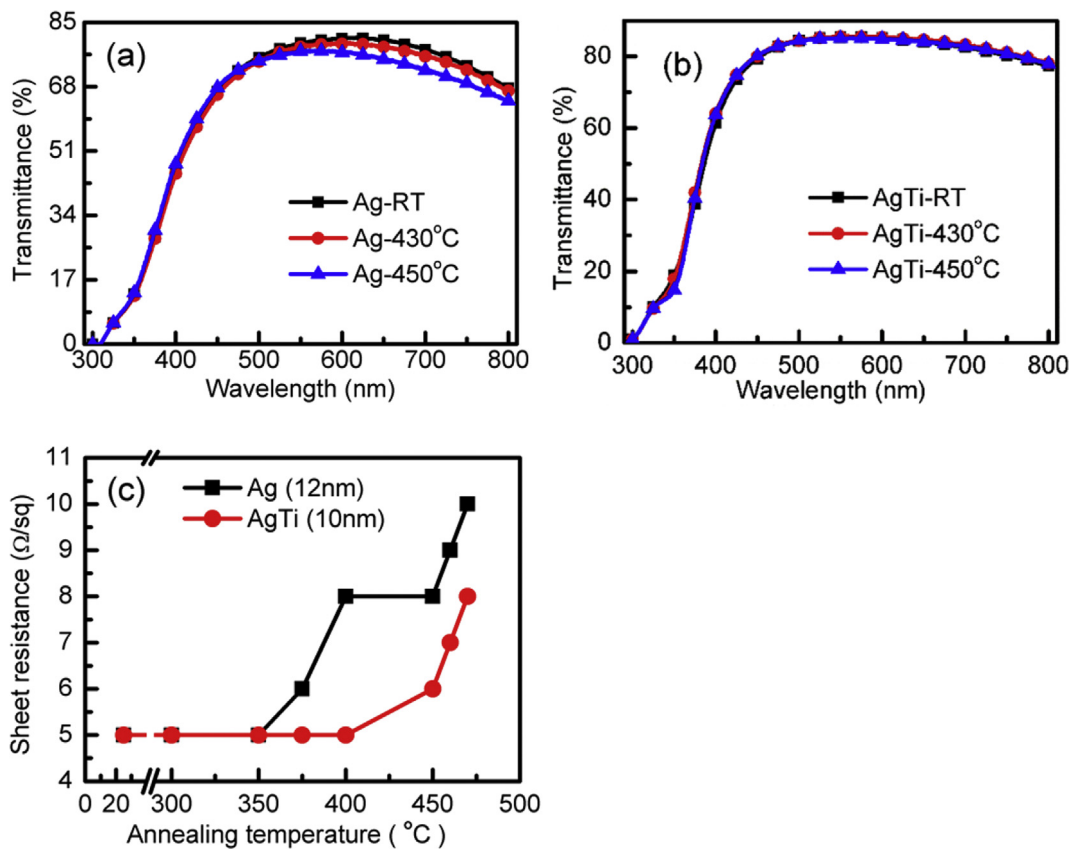


Fig. 2. Transmittance spectra of GZO(40 nm)/Ag(12 nm)/GZO(40 nm) (a) and GZO(40 nm)/AgTi(10 nm)/GZO(40 nm) (b) with different annealing temperature. (c) Sheet resistance of GZO(40 nm)/Ag(12 nm)/GZO(40 nm) and GZO(40 nm)/AgTi(10 nm)/GZO(40 nm) with different annealing temperature for 30 min.

plasmonic effect of Ag films. The inserted Ag nanostructure film shows the typical plasmonic resonance wavelength range from 500 nm to 800 nm, which is related to the morphologies, sizes, and arrangements of metal nanoparticles [12,33]. Therefore, the optical transmittance variance of GAG film in the wavelength range from 500 nm to 800 nm is more sensitive than that of the short wavelength when the morphologies of Ag nanostructures were changed under annealing condition. The sheet resistance of GAG and GATG films with different annealing temperature was shown in Fig. 2c. The sheet resistance of GAG and GATG films was slightly decreased under annealing at less than 300 °C for 30 min in air. The sheet resistance of GATG still keep stable under annealing at 400 °C,

while the sheet resistance of GAG film was obviously increased to ~8 Ω/sq from ~5 Ω/sq, indicating the partly continuous structures of Ag nanostructure film have been broken due to the aggregation of Ag atoms. However, the sheet resistance of GATG film still keep ~5 Ω/sq under annealing at 400 °C, indicating that the Ti doped Ag nanostructure films have better thermal stability. The results suggested that the sheet resistance compared to the optical transmittance of OMO transparent film is a more sensitive parameter to apperceive the morphology variance of inserted metal nanostructure film.

The better thermal stability of AgTi nanostructure film compared to Ag was further observed with FESEM images, as

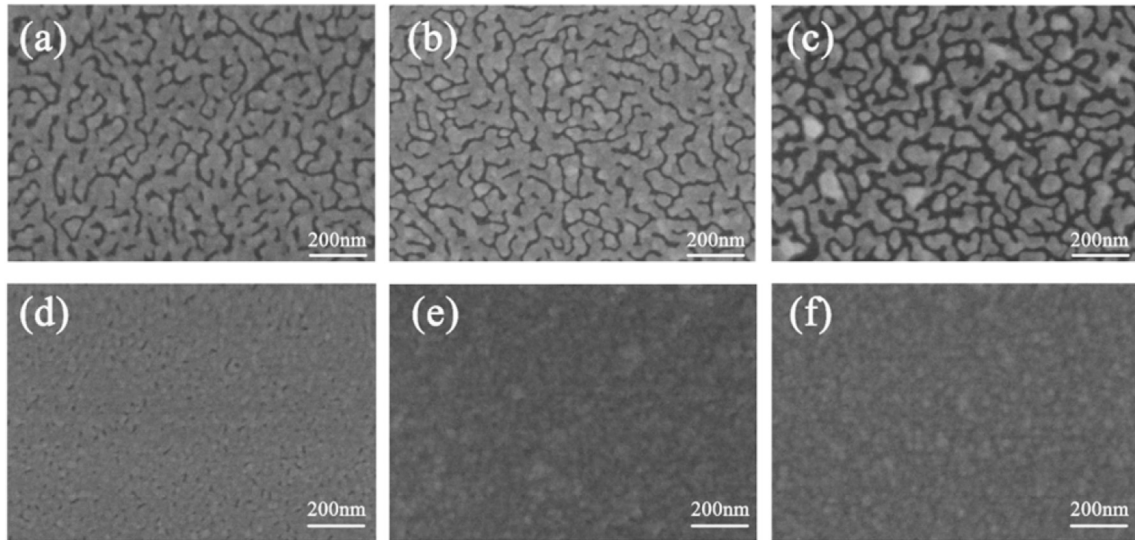


Fig. 3. FESEM images of 12 nm Ag film depositing onto GZO (40 nm) with annealing temperatures at (a) Room temperature (RT), (b) 100 °C and (c) 150 °C for 30 min in Ar filled glovebox; and 10 nm AgTi film depositing onto GZO (40 nm) with annealing at (d) RT, (e) 100 °C and (f) 150 °C for 30 min in Ar filled glovebox.

shown in Fig. 3. The 12 nm thick AgTi film have formed the quasi-continuous film, but the corresponding Ag film just forms a network film, suggesting that the nucleation of AgTi compared to that of Ag is more easily formed and have lower diffusion rate of Ag atoms. The stable morphologies of AgTi film were observed, but the aggregation effect of Ag film can be further enhanced under annealing at 150 °C due to the surface self-melting effect [34]. According to the binary alloy phase diagram, the Ag-rich AgTi alloy can only contain approximately 2 at.% Ti at 600 °C [35], which is obviously lower solubility than that (10 at.%) of Al at 200 °C in Ag-rich AgAl alloy [36]. It is not clear what Ti content is possible at room temperature but may be expected to further lower Ti solubility in Ag-rich AgTi alloy. It was found that the aggregation of Ag atoms can be obviously inhibited at even 0.1 at.% Al content in AgAl alloy [36]. The Al or Al rich phase precipitates at the grain boundaries and at the interface and easily forms Al oxide because the free energy of forming Al oxide is -889.5 kJ/mol . The forming AlO_x has been demonstrated to inhibit the aggregation and diffusion of Ag atoms [26,36]. Therefore, it is reasonably expected that Ti oxide can be more easily formed at the Ag-rich grain boundaries and the interface of AgTi film during sputtering and annealing because Ti compared to Al element has larger free energy (-1582.3 kJ/mol) of

forming Ti oxide and lower solubility in Ag-rich alloy. The Ag-rich AgTi alloy doping Ti content range from 0.2 at.% to 1.4 at.% has been demonstrated to suppress agglomeration of Ag films [26], which is consistent with our observed results. Therefore, the enhanced thermal stability of GATG film is attributed to the formation of TiO_x at the Ag-rich grain boundaries and the interface of AgTi film, which inhibit diffusion and aggregation of Ag atoms. The Ti oxide formed at the interface lowers the surface energy and increases the nucleation density of Ag film, which can easily form the smooth and continuous AgTi film [36]. The smooth and continuous metal film compared to rough and network-shape metal film helps to decrease electron scattering and improve electron transport ability. This is the reason that the sheet resistance of GATG film inserted with 10 nm thick AgTi is comparable to that of GAG film inserted with 12 nm thick Ag film under without annealing condition.

To investigate the effect of GATG substituting ITO electrode on the performance of PSCs, we fabricated two types of cells. Fig. 4 show the J-V curves of inverted PSCs with GATG and ITO electrode. The parameters of the inverted PSCs with GATG and ITO electrodes are summarized in Table 1. The V_{OC} and fill factor (FF) and J_{SC} of PSCs with GATG electrode are 0.78 V, 69.56% and 16.96

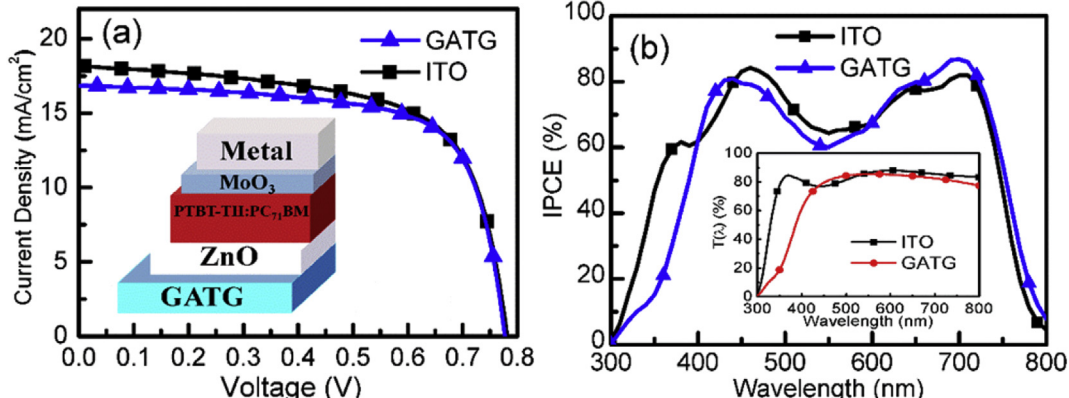


Fig. 4. (a) J-V curves of PSCs based on GATG and ITO electrodes. (b) IPCE of PSCs based on GATG and ITO electrode. Insert are the structure of PSC, and transmittance spectra of ITO and GATG electrodes, respectively.

Table 1

Parameters of PSCs with GATG and ITO electrodes.

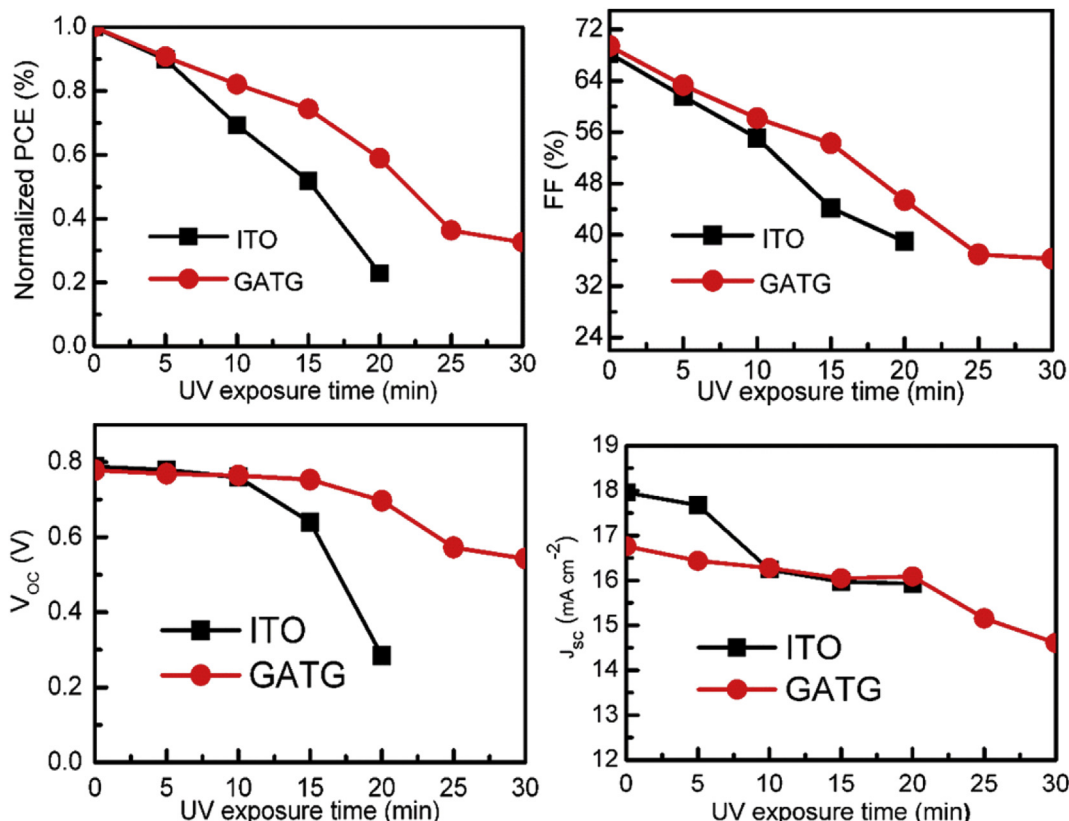
Electrode	V _{oc} (V)	J _{sc} (mA/cm ²)	FF(%)	PCE (%)
GATG	0.78	16.96	69.56	9.20 ± 0.2
ITO	0.78	18.12	65.17	9.23 ± 0.2

mA/cm², respectively. The slightly low J_{sc} of PSCs with GATG electrode compared to ITO is possibly partly attributed to the low transmittance with the wavelength of less than 380 nm. PSCs fabricated with GATG electrode reach PCE of 9.20%, which is comparable to PCE (9.23%) of PSCs with ITO electrode. Fig. 4b shows the IPCE curves of PSCs with GATG and ITO electrode. The IPCE values of PSCs with GATG electrode compared to ITO at the short wavelength side were obviously decreased, which corresponds to the cutoff in T(λ) of GATG/glass, as shown in the insert Fig. 4b. This suggests that GATG electrode can obviously block the UV portion of the solar irradiation.

The solar cells containing organic materials or groups, for examples, polymer solar cells [37] and perovskite solar cells [38] can be quickly deteriorated under the UV exposure and moisture encroachment. A right encapsulation can reduce the influences of moisture and oxygen. The UV filter covered the front side of PSCs can usually eliminate UV-induced degradation of cells by preventing UV light in solar irradiance reaching the active region [9]. However, the additional UV-filter would increase manufacturing process and cost of PSCs. The poor transparency in UV range of GATG film, as shown in insert Fig. 4b, is expected to play the role of UV-filter. UV-assisted acceleration aging test of PSCs with relative humidity (RH) of 68% in air was carried out to evaluate UV durability of cells. The parameters of PSCs with GATG and ITO electrodes with different UV irradiation time are shown in Fig. 5. The

parameters including PCE, FF, J_{sc}, and V_{oc} of the inverted PSCs with ITO was more quickly deteriorated under UV-assisted acceleration aging test. The normalized PCE of the control PSC with ITO electrode was decreased to 23% of the original PCE value under UV exposure for 20 min. However, PSCs with GATG electrode still remain 59% of the original PCE value, indicating that GATG-based PSCs exhibit distinctive enhancement in the UV durability due to low transparency of GATG electrode in the UV wavelength range.

It was observed that the parameters of FF and V_{oc} compared to J_{sc} of PSCs show more easily deterioration under UV exposure. The maximum achievable V_{oc} of organic solar cells is determined by the offset between the quasi-Fermi levels of the photoinduced hole (E_{F,h}) in the donor and the photoinduced electrons (E_{F,e}) in the acceptor. The V_{oc} would be reduced when the contact interfaces between electron/hole transport layers and active layer are deteriorated. And the contact interfaces between electron/hole selective layers and electrodes can also influence the V_{oc} of organic solar cells [24]. The degradation pathways of PSCs usually include chemical degradation of PTB7-Th:PC₇₁BM active layer, interfacial materials, electrodes and their interfaces. Fig. 6a and b shows absorption spectra of PTB7-Th:PC₇₁BM active layer spin-coated onto ZnO/ITO and ZnO/GATG surfaces under different UV exposure time. The relative absorption of wavelength range from 600 nm to 750 nm of PTB7-Th:PC₇₁BM active layer onto ZnO/ITO compared to ZnO/GATG surface was more quickly weaken under UV exposure. Furthermore, the absorption peaks of the active layer onto ZnO/ITO and ZnO/GATG surface were respectively blue-shifted to 700 nm and 709 nm from 712 nm under UV exposure for 10 min. The absorption of the wavelength range from 600 nm to 750 nm is primarily attributed to PTB7-Th polymer and the absorption peak of 712 nm originates from PTB7-Th [39]. The obviously blue-shifted absorption peak indicates that the conjugated bonds of PTB7-Th

**Fig. 5.** Normalized PCE, FF, V_{oc} and J_{sc} of inverted PSCs with ITO and GATG transparent electrodes under different UV exposure time with RH 68% in air.

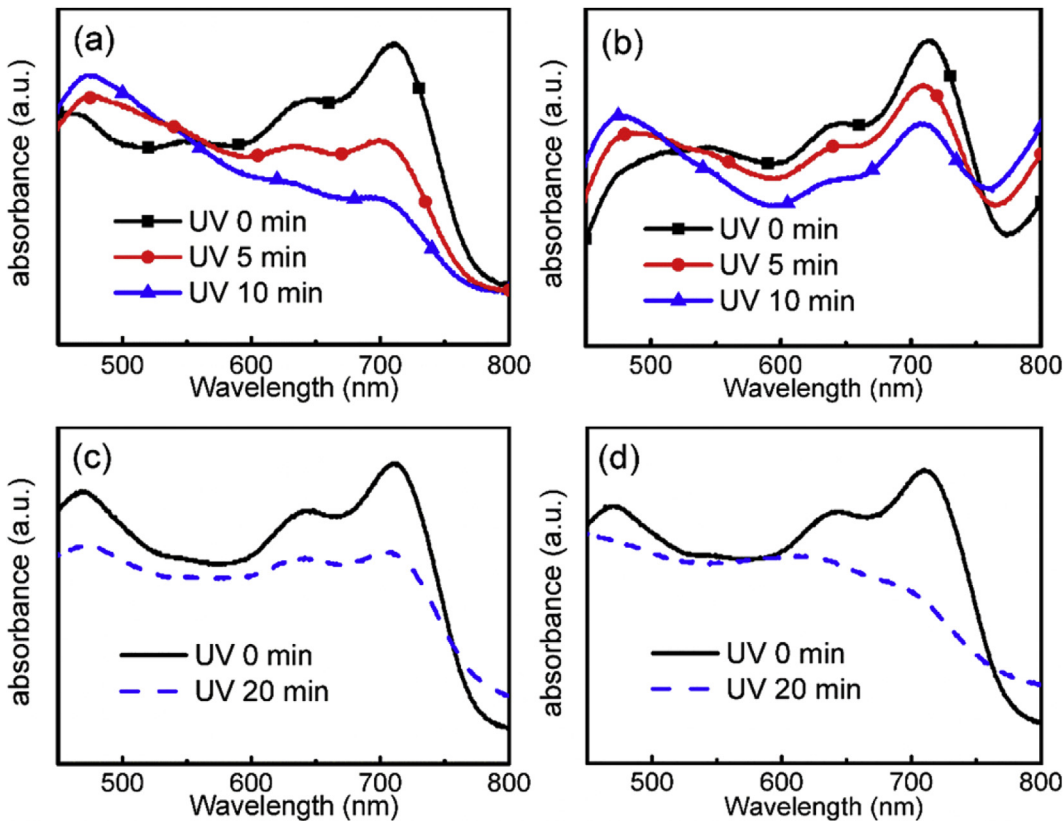


Fig. 6. Absorption spectra of PTB7-Th:PC₇₁BM active layer spin-coated onto ZnO/ITO/glass (a), ZnO/GATG/glass (b), glass (c) and ZnO/glass (d) under different UV exposure time.

polymer was partly broken under UV exposure. This is because the broken conjugated bonds can limit the interchain charge-transfer state and change the energy levels of the highest occupied molecular orbital (HOMO) and the lowest unoccupied molecular orbital (LUMO) [40]. Therefore, we can conclude that the anti-UV ability of PTB7-Th polymer can be increased under the protection of GATG films. The performance of solar cells with TiO₂ as an electron transport layer can be quickly deteriorated under UV exposure because TiO₂ material has photocatalytic function [41]. Similar to TiO₂, ZnO material also has certain photocatalytic effect [42]. The absorption spectra of PTB7-Th:PC₇₁BM active layer without and with ZnO layer under different UV exposure time are shown in Fig. 6c and d. The absorption peak of 712 nm almost disappears for the active layer onto ZnO/glass under UV exposure for 20 min, indicating that the PTB7-Th polymer was obviously deteriorated compared to PTB7-Th:PC₇₁BM directly spin-coated onto glass due to the photocatalytic effect of ZnO layer. Therefore, we can reasonably expect that the active material closing to the interface of ZnO layer has faster decay rate compared to bulk inner active material under UV exposure, which can reduce the V_{oc} due to the faster deterioration of the interface contact between electron transport layer and active layer. The traps states of the active layer produced under the UV-assisted photo-oxidation and photo-degradation can greatly increase recombination of carriers, which result in the low FF value and photocurrent. Therefore, GATG substituting ITO as an electrode can serve as a UV filter to inhibit UV degradation of PSCs.

4. Conclusions

In conclusion, GATG transparent conducting film with low sheet resistance and high optical transmittance were fabricated by the

magnetron sputtering method. The thermal stability of the GATG film compared to GAG film was significantly improved due to the formation of TiO_x, which can inhibit the aggregation of Ag atoms. PSCs with GATG electrode attained a PCE of 9.20%, which is comparable to that of the control PSCs with ITO. Furthermore, PSCs with GATG compared to ITO can obviously enhance the UV durability. These results suggest that the GATG as an alternative to ITO electrode has potential advantage to enhance anti-UV ability of PSCs, which can save UV-filter and the cost, and simplify the fabrication process of PSCs.

Acknowledgments

This work was supported by National Natural Science Foundation of China (grant Nos. 61275038 and 11274119).

References

- [1] Z. He, C. Zhong, S. Su, M. Xu, H. Wu, Y. Cao, Enhanced power-conversion efficiency in polymer solar cells using an inverted device structure, *Nat. Photonics* 6 (2012) 593–597.
- [2] H.-K. Park, J.-W. Kang, S.-I. Na, D.-Y. Kim, H.-K. Kim, Characteristics of indium-free GZO/Ag/GZO and AZO/Ag/AZO multilayer electrode grown by dual target DC sputtering at room temperature for low-cost organic photovoltaics, *Sol. Energy Mater. Sol. Cells* 93 (2009) 1994–2002.
- [3] C. Jiang, Q. Jiang, J. Lu, Z. Ye, Structural, optical and electrical properties of Ga doped ZnO/Cu grid/Ga doped ZnO transparent electrodes, *J. Mater. Sci. Technol.* 31 (2015) 1108–1110.
- [4] F.C. Krebs, All solution roll-to-roll processed polymer solar cells free from indium-tin-oxide and vacuum coating steps, *Org. Electron.* 10 (2009) 761–768.
- [5] S. Choi, Y. Zhou, W. Haske, J.W. Shim, C. Fuentes-Hernandez, B. Kippelen, ITO-free large-area flexible organic solar cells with an embedded metal grid, *Org. Electron.* 17 (2015) 349–354.
- [6] S. Chen, M.E.A. Warwick, R. Binions, Effects of film thickness and thermal treatment on the structural and opto-electronic properties of Ga-doped ZnO

- films deposited by sol–gel method, *Sol. Energy Mater. Sol. Cells* 137 (2015) 202–209.
- [7] M. Mickan, U. Helmersson, H. Rinnert, J. Ghanbaja, D. Muller, D. Horwat, Room temperature deposition of homogeneous, highly transparent and conductive Al-doped ZnO films by reactive high power impulse magnetron sputtering, *Sol. Energy Mater. Sol. Cells* 157 (2016) 742–749.
- [8] Y. Wang, X. Zhang, X. Meng, Y. Cao, F. Yang, J. Nan, Q. Song, Q. Huang, C. Wei, J. Zhang, Y. Zhao, Simulation, fabrication, and application of transparent conductive Mo-doped ZnO film in a solar cell, *Sol. Energy Mater. Sol. Cells* 145 (2016) 171–179.
- [9] H. Liu, Z. Wu, J. Hu, Q. Song, B. Wu, H. Lam Tam, Q. Yang, W. Hong Choi, F. Zhu, Efficient and ultraviolet durable inverted organic solar cells based on an aluminum-doped zinc oxide transparent cathode, *Appl. Phys. Lett.* 103 (2013) 043309.
- [10] S. Yu, W. Zhang, L. Li, D. Xu, H. Dong, Y. Jin, Optimization of SnO₂/Ag/SnO₂ tri-layer films as transparent composite electrode with high figure of merit, *Thin Solid Films* 552 (2014) 150–154.
- [11] K. Jeon, H. Youn, S. Kim, S. Shin, M. Yang, Fabrication and characterization of WO₃/Ag/WO₃ multilayer transparent anode with solution-processed WO₃ for polymer light-emitting diodes, *Nanoscale Res. Lett.* 7 (2012) 1–7.
- [12] L. Zhou, X. Chen, F. Zhu, X. Sun, Z. Sun, Improving temperature-stable AZO–Ag–AZO multilayer transparent electrodes using thin Al layer modification, *J. Phys. D Appl. Phys.* 45 (2012) 505103.
- [13] S.-W. Cho, Y.T. Kim, W.H. Shim, S.-Y. Park, K.-D. Kim, H.O. Seo, N.K. Dey, J.-H. Lim, Y. Jeong, K.H. Lee, Y.D. Kim, D.C. Lim, Influence of surface roughness of aluminum-doped zinc oxide buffer layers on the performance of inverted organic solar cells, *Appl. Phys. Lett.* 98 (2011) 023102.
- [14] L. Gong, J. Lu, Z. Ye, Transparent conductive Ga-doped ZnO/Cu multilayers prepared on polymer substrates at room temperature, *Sol. Energy Mater. Sol. Cells* 95 (2011) 1826–1830.
- [15] C. Chien-Hsun, W. Hung-Wei, H. Jow-Lay, Effect of annealing temperature and atmosphere on aluminum-doped ZnO/Au/aluminum-doped ZnO thin film properties, *Thin Solid Films* 605 (2015) 121–128.
- [16] S.-B. Heo, J.-H. Jeon, T.-K. Gong, H.J. Moon, S.-K. Kim, B.-C. Cha, J.-H. Kim, U.-C. Jung, S. Park, D. Kim, Influence of a Ni interlayer on the optical and electrical properties of trilayer GZO/Ni/GZO films, *Ceram. Int.* 41 (2015) 9668–9670.
- [17] T.-C. Lin, W.-C. Huang, F.-C. Tsai, The electro-optical characteristics of AZO/Mo/AZO transparent conductive film, *J. Mater. Sci. Mater. Electron.* 26 (2015) 3685–3690.
- [18] M.Y. Kim, K.T. Son, D. Lim, Effect of an Ag insertion layer on the optical and electrical properties of Ga doped zinc oxide films, *J. Nanosci. Nanotechnol.* 15 (2015) 2478–2481.
- [19] T. Winkler, H. Schmidt, H. Flügge, F. Nikolayzik, I. Baumann, S. Schmale, T. Weimann, P. Hinze, H.-H. Johannes, T. Rabe, S. Hamwi, T. Riedl, W. Kowalsky, Efficient large area semitransparent organic solar cells based on highly transparent and conductive ZTO/Ag/ZTO multilayer top electrodes, *Org. Electron.* 12 (2011) 1612–1618.
- [20] R. Pandey, C.H. Wie, X. Lin, J.W. Lim, K.K. Kim, D.K. Hwang, W.K. Choi, Fluorine doped zinc tin oxide multilayer transparent conducting Oxides for organic photovoltaic's Cells, *Sol. Energy Mater. Sol. Cells* 134 (2015) 5–14.
- [21] C.-H. Lee, R. Pandey, B.-Y. Wang, W.-K. Choi, D.-K. Choi, Y.-J. Oh, Nano-sized indium-free MTO/Ag/MTO transparent conducting electrode prepared by RF sputtering at room temperature for organic photovoltaic cells, *Sol. Energy Mater. Sol. Cells* 132 (2015) 80–85.
- [22] C. Tao, G. Xie, C. Liu, X. Zhang, W. Dong, F. Meng, X. Kong, L. Shen, S. Ruan, W. Chen, Semitransparent inverted polymer solar cells with MoO₃/Ag/MoO₃ as transparent electrode, *Appl. Phys. Lett.* 95 (2009) 053303.
- [23] Y.-S. Park, H.-K. Kim, S.-W. Kim, Thin Ag layer inserted GZO multilayer grown by roll-to-roll sputtering for flexible and transparent conducting electrodes, *J. Electrochem. Soc.* 157 (2010) J301–J306.
- [24] Z. Jiang, X. Chen, X. Lin, X. Jia, J. Wang, L. Pan, S. Huang, F. Zhu, Z. Sun, Amazing stable open-circuit voltage in perovskite solar cells using AgAl alloy electrode, *Sol. Energy Mater. Sol. Cells* 146 (2016) 35–43.
- [25] X. Jia, Z. Jiang, X. Chen, J. Zhou, L. Pan, F. Zhu, Z. Sun, S. Huang, Highly efficient and air stable inverted polymer solar cells using LiF-modified ITO cathode and MoO₃/AgAl alloy anode, *ACS Appl. Mater. Interfaces* 8 (2016) 3792–3799.
- [26] M. Kawamura, Z. Zhang, R. Kiyono, Y. Abe, Thermal stability and electrical properties of Ag–Ti films and Ti/Ag/Ti films prepared by sputtering, *Vacuum* 87 (2013) 222–226.
- [27] Z. Lu, X. Chen, J. Zhou, Z. Jiang, S. Huang, F. Zhu, X. Piao, Z. Sun, Performance enhancement in inverted polymer solar cells incorporating ultrathin Au and LiF modified ZnO electron transporting interlayer, *Org. Electron.* 17 (2015) 364–370.
- [28] W. Cheng, Z. Wu, S. Wen, B. Xu, H. Li, F. Zhu, W. Tian, Donor–acceptor copolymers incorporating polybenzo[1,2-b:4,5-b']dithiophene and tetrazine for high open circuit voltage polymer solar cells, *Org. Electron.* 14 (2013) 2124–2131.
- [29] S. Song, T. Yang, Y. Xin, L. Jiang, Y. Li, Z. Pang, M. Lv, S. Han, Effect of GZO thickness and annealing temperature on the structural, electrical and optical properties of GZO/Ag/GZO sandwich films, *Curr. Appl. Phys.* 10 (2010) 452–456.
- [30] H.-W. Wu, R.-Y. Yang, C.-M. Hsiung, C.-H. Chu, Influence of Ag thickness of aluminum-doped ZnO/Ag/aluminum-doped ZnO thin films, *Thin Solid Films* 520 (2012) 7147–7152.
- [31] J.-A. Jeong, H.-K. Kim, M.-S. Yi, Effect of Ag interlayer on the optical and passivation properties of flexible and transparent Al₂O₃/Ag/Al₂O₃ multilayer, *Appl. Phys. Lett.* 93 (2008) 033301.
- [32] H.-K. Park, J.-A. Jeong, Y.-S. Park, S.-I. Na, D.-Y. Kim, H.-K. Kim, Room-temperature indium-free Ga:ZnO/Ag/Ga:ZnO multilayer electrode for organic solar cell applications, *Electrochim. Solid State Lett.* 12 (2009) H309.
- [33] X. Chen, C. Zhao, L. Rothberg, M.-K. Ng, Plasmon enhancement of bulk heterojunction organic photovoltaic devices by electrode modification, *Appl. Phys. Lett.* 93 (2008) 123302.
- [34] X. Sun, X. Chen, Z. Zhang, Z. Sun, Plasmon based antireflection coatings containing nanostructured Ag and silica medium, *Appl. Surf. Sci.* 258 (2012) 3785–3788.
- [35] J. Murray, K. Bhansali, The Ag–Ti (Silver–Titanium) system, *Bull. Alloy Phase Diagr.* 4 (1983) 178.
- [36] K. Sugawara, M. Kawamura, Y. Abe, K. Sasaki, Comparison of the agglomeration behavior of Ag(Al) films and Ag(Au) films, *Microelectron. Eng.* 84 (2007) 2476–2480.
- [37] M. Prosa, M. Tessarolo, M. Bolognesi, O. Margeat, D. Gedefaw, M. Gaceur, C. Videlot-Ackermann, M.R. Andersson, M. Muccini, M. Seri, J. Ackermann, Enhanced ultraviolet stability of air-processed polymer solar cells by Al doping of the ZnO interlayer, *ACS Appl. Mater. Interfaces* 8 (2016) 1635–1643.
- [38] R.K. Misra, S. Aharon, B. Li, D. Mogilyansky, I. Visoly-Fisher, L. Etgar, E.A. Katz, Temperature- and component-dependent degradation of perovskite photovoltaic materials under concentrated sunlight, *J. Phys. Chem. Lett.* 6 (2015) 326–330.
- [39] S.H. Liao, H.J. Jhuo, Y.S. Cheng, S.A. Chen, Fullerene derivative-doped zinc oxide nanofilm as the cathode of inverted polymer solar cells with low-bandgap polymer (PTB7-Th) for high performance, *Adv. Mater* 25 (2013) 4766–4771.
- [40] X. Chen, Z. Wang, Y. Hou, Z. Xu, X. Xu, Photoluminescence quenching in poly(p-phenylene vinylene) derivative, *Displays* 21 (2000) 55–60.
- [41] W. Li, W. Zhang, S. Van Reenen, R.J. Sutton, J. Fan, A.A. Haghighirad, M.B. Johnston, L. Wang, H.J. Snaith, Enhanced UV-light stability of planar heterojunction perovskite solar cells with caesium bromide interface modification, *Energy Environ. Sci.* 9 (2016) 490–498.
- [42] X. Liu, L. Pan, J. Li, K. Yu, Z. Sun, C.Q. Sun, Light down-converting characteristics of ZnO-Y2O2S: Eu³⁺ for visible light photocatalysis, *J. Colloid Interface Sci.* 404 (2013) 150–154.